Robust Control of a Flexible-Hull Propulsion System

by

Christopher D. Gadda

Submitted to the Department of Electrical Engineering and Computer Science
in partial fulfillment of the requirements for the degrees of

Bachelor of Science in Electrical Engineering
and

Master of Engineering in Electrical Engineering and Computer Science
at the

Massachusetts Institute of Technology

May 22, 1998
[June 1998]

Author.....
Department of Electrical Engineering and Computer Science
May 22,1998

Approved by.....
Dr. Jamie Anderson
Senior Member, Technical Staff, Charles Stark Draper Laboratory
Thesis Supervisor

Certified by.....
Professor Jean-Jacques Slotine
Professor, Massachusetts Institute of Technology
Thesis Supervisor

Accepted by.....
Professor Arthur C. Smith
Chairman, Department Committee on Graduate Theses

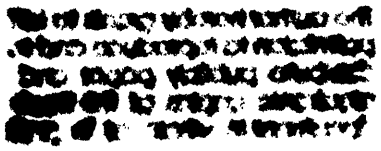

Robust Control of a Flexible-Hull Propulsion System

by

Christopher D. Gadda

Submitted to the
Department of Electrical Engineering and Computer Science

May 29, 1998

in partial fulfillment of the requirements for the degrees of
Bachelor of Science in Electrical Engineering
and Master of Engineering in Electrical Engineering and Computer Science

ABSTRACT

The Charles Stark Draper Laboratory is continuing the research done on fish-like propulsion systems with the Vorticity Control Unmanned Underwater Vehicle (VCUUV) project. The VCUUV is a fully autonomous robotic fish, which employs a flexible tail structure for propulsion and maneuvering. This paper describes the design, implementation, and testing of a control system for the tail of the VCUUV. Both linear and nonlinear control techniques are discussed.

Thesis Supervisor: Jamie Anderson
Title: Senior Member, Technical Staff, Charles Stark Draper Laboratory

Thesis Supervisor: Jean-Jacques Slotine
Title: Professor, Massachusetts Institute of Technology

ACKNOWLEDGEMENTS

May 29, 1998

This thesis was prepared at The Charles Stark Draper Laboratory, Inc., under Internal Research and Development funding.

The computer rendered images in this document were created by Alan DiPietro.
MATLAB and Simulink are registered trademarks of The Mathworks, Inc.

I would like to thank Professor Slotine for his assistance with this project. I would also like to thank Dr. Jamie Anderson and the members of the VCUUV team for their efforts and for making this exciting project possible. I would like to give special thanks to Abigail Vargus for her support and hours of assistance editing this thesis.

ASSIGNMENT

Draper Laboratory Report Number T_____

In consideration for the research opportunity and permission to prepare my thesis by and at The Charles Stark Draper Laboratory, Inc., I hereby assign my copyright of the thesis to The Charles Stark Draper Laboratory, Inc., Cambridge, Massachusetts.

..... 5/29/98

Christopher D. Gadda (date)

CONTENTS

LIST OF FIGURES

LIST OF TABLES

1. INTRODUCTION

The efficiency with which fish are able to propel themselves has drawn significant attention from the research community in recent years. In conjunction with the high degree of maneuverability that fish posses, fish-like propulsion techniques show real potential for replacing conventional propeller-based propulsion systems in many applications. Several research projects have endeavored to create underwater robots capable of fish-like propulsion, to study its advantages and disadvantages.

The first of these projects, "RoboTuna," demonstrated a substantial increase in propulsive efficiency. The RoboTuna project was used to determine and study the optimal tail trajectories for propulsion of tuna-shaped vehicles. However, RoboTuna was constrained by an overhead track which allowed travel in only one dimension. This constraint limited the project's usefulness for studying maneuverability.

The Charles Stark Draper Laboratory is continuing the research in flexible-hull propulsion systems with the Vorticity Control Unmanned Underwater Vehicle (VCUUV) project. This first chapter provides an overview of the VCUUV project and its goals and acquaints the reader with the structure and content of this thesis.

1.1. VCUUV Project Overview

The purpose of the Vorticity Control Unmanned Underwater Vehicle (VCUUV) Project is to continue the study of the efficiencies of fish-like propulsion, to research various techniques for acceleration using vorticity control, and to demonstrate the fitness of flexible-hull propulsion systems for use with autonomous underwater vehicles.

When the VCUUV is completed, there will be several control loops in operation all of the time. Control loops will maintain the position of the tail, the pressure of the hydraulic fluid, and the depth, heading, and velocity of the vehicle. The scope of this thesis, however, is limited to the system responsible for positioning the tail.

1.2. Thesis Overview

The focus of this thesis is the design and analysis of the control system for the tail portion of the VCUUV. A brief description of the succeeding chapters is provided here to clarify the scope and direction of this thesis.

Chapter two, *Control System Requirements*, discusses the specific constraints and specifications of the control system. This chapter includes a description of the plant and its operating environment, assesses the bandwidth requirements of the control system, and discusses how to measure the performance of the control system.

Chapter three, *Models,* describes the development of the mathematical models of the plant. The approximations made in developing the models and their anticipated effects on system stability and performance are discussed.

Chapter four, *Linear Position Control Techniques*, discusses the design of a control system using traditional linear control techniques, such as proportional control and simple linear variations thereof. This chapter also discusses some of the practical considerations regarding implementation of such control techniques.

Chapter five, *Nonlinear Position Control Techniques,* describes how nonlinear control techniques can be used to achieve improved control performance. The focus is, specifically, how the use of nonlinear control overcomes some errors caused by plant nonlinearities.

Chapter six, *Control System Performance Analysis,* presents an analysis of the previously described control techniques. Actual data is compared with modeled performance, and possible explanations for any discrepancies are discussed.

Chapter seven, *Conclusion,* summarizes the work completed and discusses areas for future research.

2. CONTROL SYSTEM REQUIREMENTS

It is important to understand the performance criteria which the control system must meet before beginning design. This chapter provides a brief overview of what the plant consists of, what the specific requirements for the control system are, and how the control system's performance should be assessed.

2.1. Overview

The tail structure of the VCUUV is composed of three rigid aluminum links and a caudal fin, all designed to hinge in the horizontal plane. The positions of the three links and fin are controlled by hydraulic cylinders. An outer shell made of rings of rigid foam encloses this structure. The foam rings act like ribs and are attached to a pair of flexible spines. One of the spines runs along the top of the tail, and one is located along the bottom. The "ribs" are covered in overlapping flexible scales. A thin neoprene skin covers the entire assembly. This arrangement provides a flexible hull and gives the tail the appropriate shape. A cutaway view of the entire VCUUV is shown in Figure 2-1. The arrangement of rigid links, fins, and hydraulic cylinders can be seen in Figure 2-2.

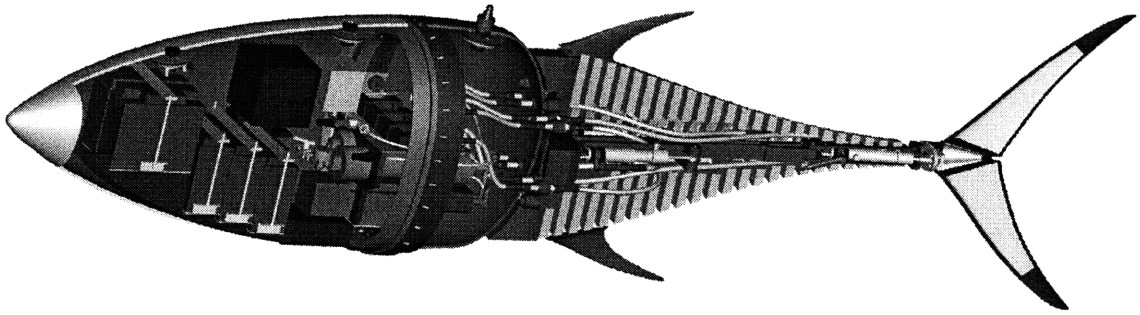

Figure 2-1 Rendered Cutaway View of the VCUUV

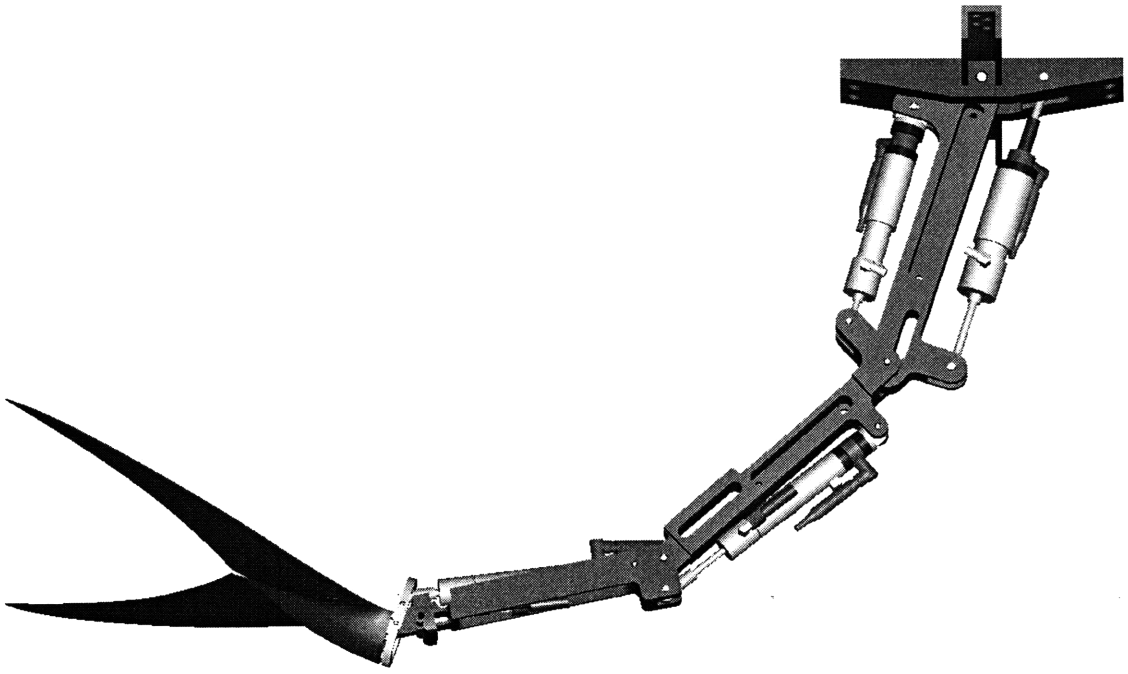

Figure 2-2 Rendered Image of Tail Assembly

Software running on the on-board processors generates a set of trajectories for the links and caudal fin. These trajectories are typically constants or sinusoids with frequencies not in excess of 1.5Hz. It is not known at this time if other types of trajectories will be required for motions such as turning, stopping, or accelerating, but the design of this control system is based on a desire to track low-frequency sinusoids.

2.2. Robustness

A robust control system continues to meet its performance constraints even when the actual system differs from the modeled one. Since it is typically not possible to know precisely the response of the plant, nor is it possible to construct a controller exactly as designed, some level of robustness is required of all control systems.

Oftentimes, better system performance can be achieved by developing a simpler model of a system and designing a robust controller which can handle the errors in the model, than by developing a more precise model and a complex controller to go with it [1].

There are several areas of uncertainty in the VCUUV control system, so robustness is an important factor in the design of the control system for the VCUUV. The dynamics of the tail is the area of greatest uncertainty in the VCUUV, worsened by the fact that sometimes the fish is operated in the water and sometimes out.

2.2.1. Operating Environment

The VCUUV must be able to operate correctly both in and out of water. Although the VCUUV is designed for underwater operation, at times it will be operated out of the water. For example, on-shore demonstrations are common and a large amount of preliminary testing is done on dry land. The dynamics of the tail structure depend on the operating environment. A control system for the tail must be robust enough to handle these changes in system dynamics and still perform correctly.

It is desirable to have a single control system which is capable of handling the changing operating environment, as opposed to having different control systems for use in air and water. A single control system will continue to work properly when the environment changes unexpectedly, such as when the VCUUV reaches the surface and part of its tail is exposed.

2.2.2. Parameter Error

When a particular control system design is actually implemented, parameter error is introduced. In continuous-time controllers this is typically the result of physical device tolerances. With discrete-time controllers parameter error arises from rounding errors on the control processor. For example, if the optimal gain for some portion of a controller is calculated to be $\sqrt{2}$, there is no way to represent this number precisely, so it must be rounded off or truncated at some point, introducing error.

2.3. Bandwidth

In designing a control system, it is always important to understand the nature of the trajectories which the control system will be required to track. It is particularly helpful to know what frequencies will be present in the trajectories so that the required bandwidth of the control system can be established.

Research in the area of fish-like propulsion systems is still in its early stages and not very much is known about the specific tail trajectories used by fish. From the work done on the RoboTuna project, optimal trajectories for straight, constant-speed swimming were determined. At this time, the optimal trajectories for actions such as acceleration, turning, and stopping are not known. The VCUUV project should result in a better understanding of what these trajectories are.

Based on results of the RoboTuna project, the theoretically optimal trajectories for straight, constant-speed swimming with the VCUUV were calculated. The motion of the tail is essentially a travelling wave whose amplitude increases toward the end of the tail. It can be shown that this motion can be achieved by controlling the relative angles between each link to follow a set of sinusoids of various amplitudes and phases.

The VCUUV is designed to swim at frequencies of up to 1.4Hz. The closed-loop bandwidth must be large enough that the attenuation at 1.4Hz is negligible. Adding an order of magnitude gives a good estimate of the minimum bandwidth required. Meeting this bandwidth guideline does not, however, guarantee correct operation of the control system, nor does it suggest that a control system with only 12Hz of bandwidth will not work. The objective is to design a control system that keeps the tracking error within acceptable limits, and this bandwidth estimation can assist in designing such a system.

2.4. Tracking Error

The difference between the desired trajectory and the actual trajectory is known as the tracking error. In the design of the control system for the VCUUV, it is desired that the tracking error in response to a particular trajectory be as small as possible. Just how

small this error must be in order for the VCUUV to operate correctly is not really known, but it is felt that tracking errors under 1% of the desired trajectory will not have a serious impact on system performance.

It is not an uncommon practice in control systems design to focus on the nature of the step response of a control system. In the case of the VCUUV this is not a very useful measure for several reasons. First of all, the trajectories used for swimming motion do not include step transitions, so the ability to follow such a waveform is not as important as it is in some control applications. Second, the model of the hydraulic system, as will be seen in chapter 3, is not linear. The linearized version of this model does not handle situations where the hydraulic system is required to output large amounts of force, such as when attempting to accelerate a mass instantaneously to track a step input. For this reason it is unreasonable to compare the modeled step response of a control system with the actual step response. Also, an attempt to track a step transition in position can create forces high enough that the tail mechanism could damage itself. Great effort has gone into creating software designed to prevent the tail from attempting step transitions.

As the trajectories which are most important to track correctly are sinusoids under 1.4Hz, these are also the trajectories best suited to use for measuring tracking error. Certainly if a control system is able to track signals containing higher frequencies as well, this is a desirable feature, but the sinusoidal trajectories under 1.4Hz are the ones which need to be followed with as little error as possible.

3. MODELS

In order to design a control system which can satisfy the requirements of chapter 2, a mathematical model of the system to be controlled must first be established. In developing the model for the VCUUV control system there are tradeoffs between accuracy and complexity, as there are with any physical system modeling problem. In many cases a highly accurate and complex model is not as useful as a simpler, less exact one because it becomes too awkward to work with. However, choosing an overly simplified model can lead to design of an inappropriate control system, so a balance must be struck.

The systems which need to be modeled in order to develop the tail control system are the hydraulic system, the mechanical and fluid dynamics of the tail assembly, the sensors and signal-conditioning hardware, and the dynamics associated with discrete-time control. This chapter presents an overview of the system to be controlled, then describes how the mathematical models for each system were developed, what approximations were made, and what impact these approximations might have on system performance.

3.1. Control System Overview

The basic structure of the control system is as follows: There is a TMS320C44 digital signal processor as the core of the controller. It controls, via a set of digital-to-analog converters, the input signal to a set of four servovalves. These servovalves regulate the rate of flow of hydraulic fluid from a high-pressure reservoir to each of four hydraulic cylinders which control the position of each link on the tail.

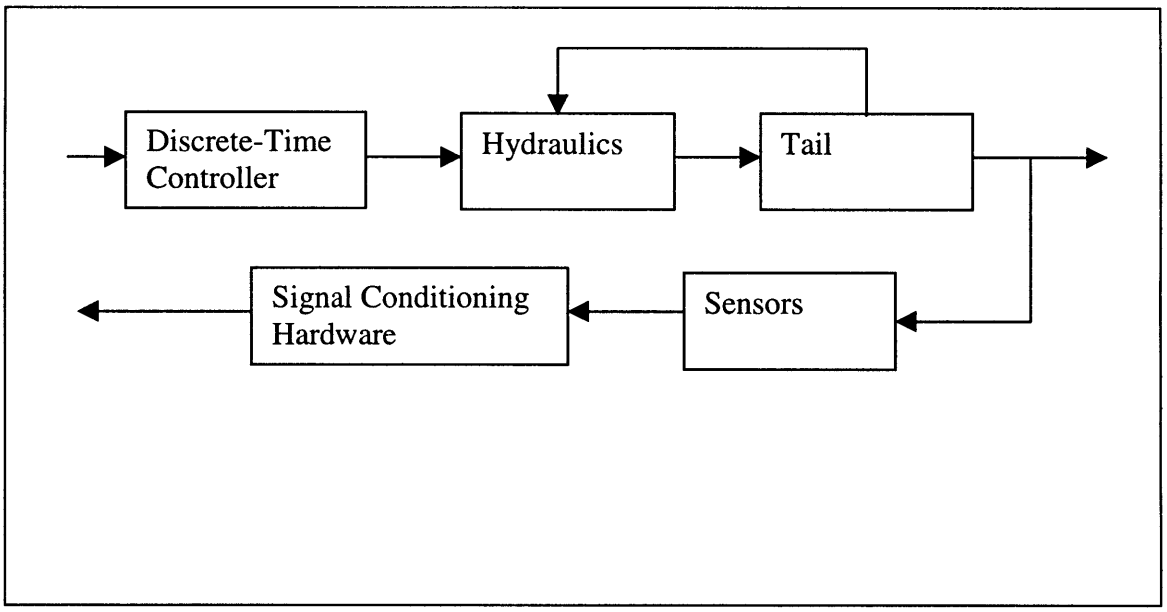

Figure 3-1 Block Diagram of Model

3.2. Tail Dynamics

Modeling the dynamics of the tail assembly presents a significant challenge. While the dynamics of the mechanical system are straightforward, the hydrodynamics of the tail as it moves through water is a complicated subject and not fully understood at this time. For this reason, it seemed more practical to focus on only the most significant components of the tail dynamics rather than try to develop a precise model.

From the results of the RoboTuna project, it was assumed that the dynamics of the tail structure would be dominated by the mass of the water inside the tail, and the added mass of the water surrounding the tail. From this assumption, the model of the tail is given by

$$f = m_{eff}\ddot{x} \tag{3.1}$$

where m_{eff} is the effective mass of a particular link of the tail. Determining the value of this effective mass is non-trivial.

First, a link of the tail is modeled as a cylinder of a radius equal to the average radius of the tail structure surrounding that particular link. The length of the cylinder is set to the length of the link. The mass of this cylinder is given by its volume times the density of water, as the tail is designed to be neutrally buoyant. This mass is then doubled to account for the added mass of the water around the outside of the tail structure. The symbol m_c is used to refer to this mass.

$$m_c = 2\pi\rho l r^2$$

(3.2)

Here ρ represents the density of water, l the length of the link, and r the average radius of the link.

The approximate moment of inertia associated with this cylinder is given by

$$I = \tfrac{1}{4} m_c r^2 + \tfrac{1}{3} m_c l^2$$

(3.3)

Over the small range of angles the tail is designed to operate, the conversion between linear cylinder position and angular link position is approximately linear. This means linear acceleration and angular acceleration can be approximately related by

$$\ddot{x} = k_a \dot{\omega}$$

(3.4)

Combining these equations and the basic laws for torque, a closed-form expression for m_{eff} is given by

$$m_{eff} = \frac{2\pi\rho(\frac{1}{4}lr^4 + \frac{1}{3}l^3r^2)}{dk_a}$$

(3.5)

where d is the distance between the pivot of a particular link and the point where the hydraulic cylinder applies force.

This equation can be used to estimate the loads a cylinder will be subjected to while tracking a particular trajectory. This derivation does not address the issues of coupling between links and hence is in no way a precise analysis of the actual loading of a particular cylinder.

3.3. Hydraulic System

This section first describes the layout of the hydraulic system and then discusses the development of a basic mathematical model used to describe its operation.

3.3.1. Description

The core of the hydraulic system consists of a motor and pump, a high-pressure accumulator, a low-pressure accumulator, four servovalves, and four cylinders. The system is designed so that the flow of hydraulic fluid from the high-pressure accumulator to the cylinder and from the cylinder to the low-pressure accumulator can be regulated by the servovalves. Further, the servovalves are designed such that high-pressure fluid can be directed to either side of the cylinder, making it possible to either extend or retract the cylinder. Figure 3-2 show a schematic diagram of the complete hydraulic system.

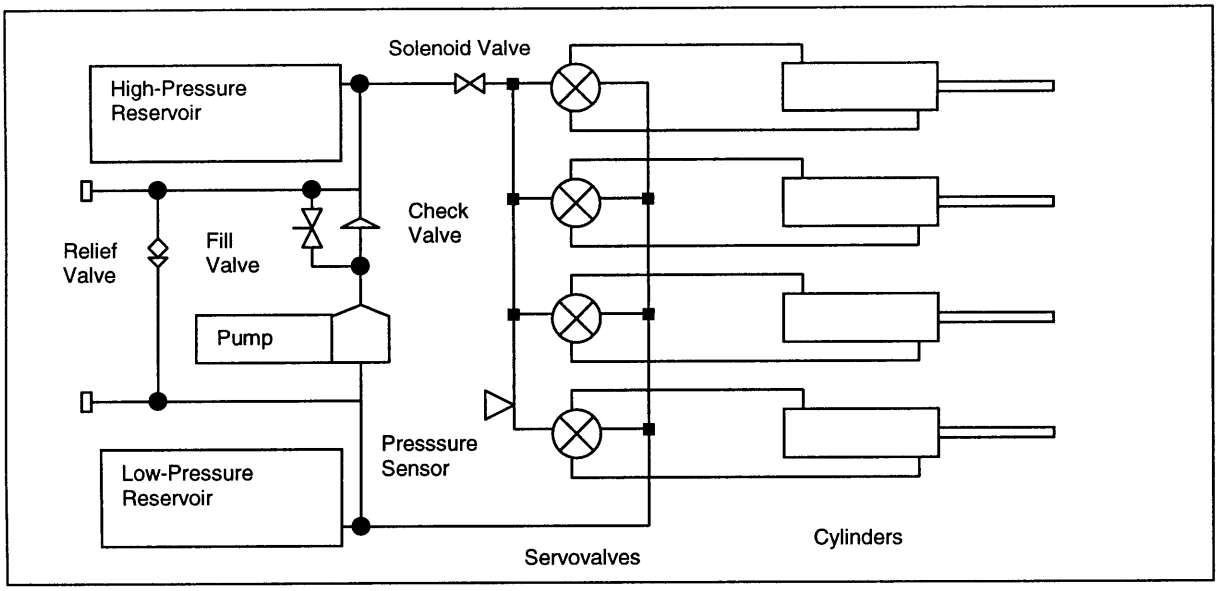

Figure 3-2 Diagram of Hydraulic System

The high-pressure accumulator is pre-charged to typically around 400 psi with nitrogen, making that the lowest pressure that can be maintained in the system. If the pressure of the hydraulic fluid falls below the pre-charged pressure, the high-pressure accumulator will be completely empty, and the pressure of the hydraulic fluid will quickly fall to zero. The low-pressure accumulator is ported to the interior of the hull which is typically pressurized to 1 atm. For this reason, unless otherwise noted, all pressures in the hydraulic system are measured relative to atmospheric pressure, assumed here to be 14 psi.

The servovalves have an operating bandwidth of 100Hz. This bandwidth exceeds the anticipated requirements of the system by nearly two orders of magnitude, meaning that the dynamics of the servovalves can essentially be ignored in developing a model for the control system. Each servovalve is bored out to a different diameter internally so that they each have a different maximum flow rate. Table 3-1 shows the flow rates for each servovalve when they are commanded to the fully open position, in either direction, with a 1000 psi pressure drop across the servovalve.

Table 3-1 Maximum Servovalve Flow Rates

Servovalve for link #1	1.8 GPM @ 1000 psi
Servovalve for link #2	.9 GPM @ 1000 psi
Servovalve for link #3	.4 GPM @ 1000 psi
Servovalve for link #4	.18 GPM @ 1000 psi

Each servovalve provides two variable-sized orifices – one between the high-pressure accumulator and the cylinder and the other between the low-pressure accumulator and the cylinder. The structure of the servovalve is such that these two orifices are always the same size. The relative flow rates through these orifices, however, are typically not equal except when there is no flow at all. This is because the flow rates are constrained by the geometry of the cylinder to which the servovalve is connected. The surface areas of the two sides of the piston inside a given cylinder are not equal because of the rod attached to one of the sides. This causes the difference in flow rate between the two sides of the cylinder.

The pump and motor assembly move fluid from the low-pressure accumulator to the high-pressure accumulator through the check valve. The check valve prevents fluid from back-driving the pump when the motor is not on. In practice, the check valve sometimes fails to perform this function properly, but the rate at which the pump runs backward is typically slow enough that this is not a serious concern.

The solenoid valve is included as a safety feature, so that in the event of an unexpected system shutdown, the high-pressure accumulator is isolated from the servovalve manifold, preventing any further tail movement. Additionally, when the servovalve controllers are powering up or shutting down, the position of the servovalve becomes undefined, so the solenoid valve is always kept closed during either of the conditions, again preventing unexpected and possibly dangerous tail movements.

The relief valve is designed to prevent the pressure in the high-pressure accumulator from exceeding a safe level, even if the pump continues to run. This prevents a possible rupture in the event of software malfunction in the pump control code, or in the event of

pressure sensor malfunction, where the sensor might report a value which is lower than the actual pressure. Another situation where the pressure relief valve is very important occurs when the solenoid valve is closed for some reason, but the pump controller is trying to maintain pressure in the hydraulic system. Since, in this scenario, the pressure sensor is isolated from the pump by the solenoid valve, the pump controller is unable to measure the pressure in the high-pressure accumulator and runs the pump continuously. The relief valve is set to open when the pressure drop across it exceeds 1200 psi. Every component in the hydraulic system is rated for at least 1500 psi, so there is a margin for error of 300 psi.

3.3.2. Model

The model of the hydraulic system takes servovalve command, high-pressure accumulator pressure, and cylinder force as its inputs and outputs cylinder position. The rate of flow through the orifices in the servovalve can be approximated by

$$q = u \times k\sqrt{\Delta P}$$

(3.6)

where q is the flow rate, k is a proportionality constant, u is the servovalve command, and ΔP is the pressure drop across the orifice.

The relative rates of fluid flow through the two halves of the servovalve are given by

$$\frac{q1}{q2} = \frac{A1}{A2}$$

(3.7)

with $q1$ and $q2$ representing the two flow rates, and $A1$ and $A2$ representing the ratio of the areas. From continuity, the relation between position and fluid flow can be established.

$$\dot{x} = \frac{q1}{A1} = \frac{q2}{A2}$$

(3.8)

By combining these equations the complete model of the hydraulic system is determined. It is interesting to note that a separate model is required for negative servovalve commands. In (3.9) P_h represents the instantaneous high-pressure accumulator pressure.

$$\dot{x} = \begin{cases} \frac{1}{A1} u \times k \sqrt{\frac{P_h - \frac{f}{A2}}{\left(\frac{A2}{A1}\right)^2 + \frac{A2}{A1}}} & u \geq 0 \\ \frac{1}{A2} u \times k \sqrt{\frac{P_h - \frac{f}{A1}}{\left(\frac{A1}{A2}\right)^2 + \frac{A1}{A2}}} & u \leq 0 \end{cases}$$

(3.9)

This expression establishes a nonlinear model for the hydraulic system. It is desirable to have a linear approximation for this model. The first step in linearizing this model is to assume the piston surface areas, $A1$ and $A2$, are approximately equal. The piston surface areas are listed in .

Table 3-2 Piston Surface Areas

Piston #	$A1$ (in^2)	$A2$ (in^2)	A (in^2)
1	.631	.785	.708
2	.319	.442	.381
3	.147	.196	.172
4	.147	.196	.172

The fourth column of Table 3-2 lists the averages of A1 and A2 for each cylinder. This average value A is used as an approximation for both A1 and A2, yielding

$$\dot{x} = \frac{1}{A\sqrt{2}} u \times k\sqrt{P_h - \frac{f}{A}}$$

(3.10)

as a greatly simplified model.

The f term is the place in this model where the dynamics of the tail factor in. If, however, the loading on the cylinders is small compared to the high-pressure accumulator pressure, that is $f/A << P_h$, then (3.10) can be further simplified to

$$\dot{x} = \frac{1}{A\sqrt{2}} u \times k\sqrt{P_h} \ .$$

(3.11)

This approximation is reasonable based on the loading analysis done in Section 3.2. This model is particularly attractive because it is linear if P_h considered to be constant. Presumably, the pressure control loop is maintaining P_h at close to a constant value, so this is not an unreasonable assumption.

When working with linear systems it is oftentimes convenient to deal with the frequency domain representation, instead of the state-space representation. Moving

(3.11) to the frequency domain provides

$$\mathrm{H_h(s)} = \frac{k}{A\sqrt{2}} \sqrt{P_h} \times \frac{1}{\mathrm{s}}.$$

(3.12)

There are some important consequences of this last approximation. First of all, the model is now linear. Also, since the f/A term has been dropped, the model is now independent of tail dynamics, so long as the condition $f/A << P_h$ is still met. This means the links can

be treated as independent, single-input-single-output (SISO) systems. This allows the design of one SISO controller, which can then be duplicated and used for each of the four links. For the remainder of this document, except where noted, it is assumed that each link is an independent system.

3.4. Signal-Conditioning Hardware

The primary responsibility of the signal-conditioning hardware is to scale and translate the voltages reported by a particular sensor such that they map into a suitable range for the analog-to-digital conversion hardware. This is accomplished using a couple of op-amps and a few judiciously selected resistors. As the frequency response for such a circuit is essentially flat for the range of frequencies we are interested in (under 15Hz), the dynamics of this portion of the signal-conditioning hardware can be safely ignored.

The signal-conditioning hardware also includes a single-pole low-pass filter for each sensor to prevent aliasing of the high frequency components of the signal. In actuality, these filters are probably not required because the only source of signals above 15Hz is from power supply noise, which is injected at every point in the circuit. It is important to include them in the system model, however, as there presence will certainly affect the overall system dynamics.

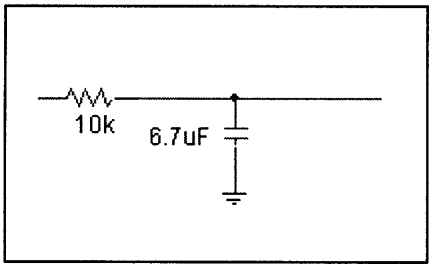

Figure 3-3 Low-Pass Filter Schematic

The circuit for these filters is shown in Figure 3-3. A frequency domain model of these filters is given by

$$H_{lp}(s) = \frac{2\pi 15}{s + 2\pi 15}$$

(3.13)

The sensors used to measure the position of the links are Digital Variable Reactance Transformers (DVRTs), chosen for their precision and waterproof packaging. According to the manufacturer's specifications, the sensors can be treated as essentially linear and with no dynamics in the frequency range in which they are operated in this application. The same is true for load sensors, which measure the force each cylinder is applying.

3.5. Discrete-Time Control System Model

The control system for the VCUUV is a discrete-time controller, which introduces additional dynamics not associated with a continuous-time controller. The advantages of discrete-time control offset this, however, allowing convenient implementation of both linear and nonlinear control techniques. There are two important aspects of discrete-time control which need to be modeled, the zero-order hold and the processing delay. Discrete-time control also introduces additional noise issues, which will be discussed in Section 3.6.

The zero-order hold is an effect of the digital-to-analog converter used in the controller. In a fixed-sampling-frequency discrete-time controller like this one, a new value for the control effort is computed on even intervals and sent to the digital-to-analog converter. In the time between receiving each value, a digital-to-analog converter acting as a zero-order hold simply continues to output the previous value. Another option, known as the first-order hold, linearly extrapolates what the output voltage should be based on the previous two values. This type of digital-to-analog converter is more expensive and thus not as common as the zero-order hold, although for certain types of signals it introduces less harmonic distortion. Figure 3-4 illustrates this difference.

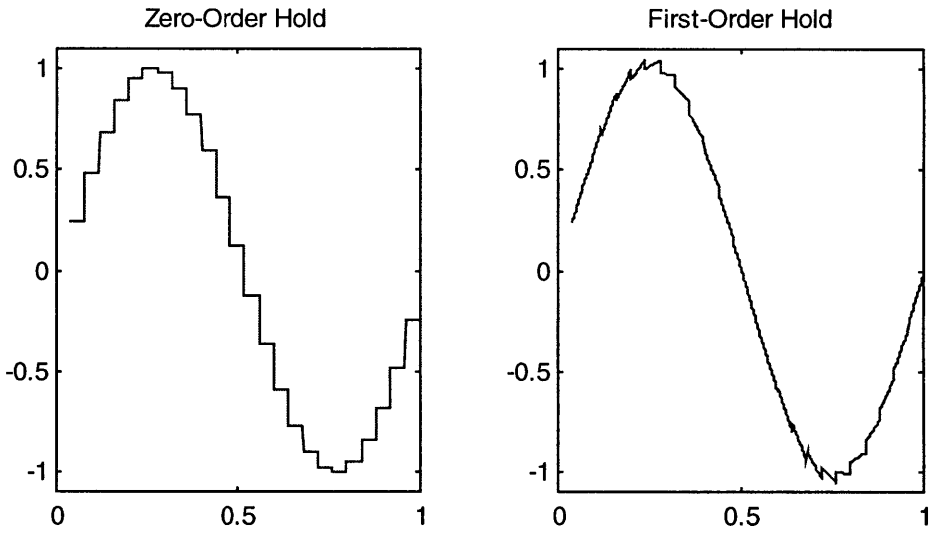

Figure 3-4 Zero-Order and First-Order Holds

The frequency domain model for a zero-order hold is given by

$$H_{z\,oh}(s) = \frac{1 - e^{-sT_s}}{s} \tag{3.14}$$

where T_s represents the sampling period. This transfer function unfortunately cannot be written as a rational expression.

The discrete-time controller always requires some non-zero amount of time to compute the next control effort value. This introduces a frequency-independent delay in the control loop. A delay in a control loop typically has a negative effect on performance and stability so it is desirable to minimize this computational delay. The software for the VCUUV is designed never to produce a computation delay larger than one sample period. To be conservative and as a matter of mathematical convenience, the computation delay is thus modeled as a one-sample delay. The frequency domain model for a one-sample delay is given by

$$H_d(s) = e^{-sT_s}$$

(3.15)

Neither (3.14) nor (3.15) can be written as a ratio of polynomials in terms of s, which makes them awkward to deal with. In particular, MATLAB handles the design, modeling, and simulation of linear systems with ease provided that the systems can be described as rational expressions. This motivates the use of the discrete-time frequency representations of the transfer functions developed so far in this chapter.

3.6. Noise

A control system needs to continue to function correctly even in the presence of noise as no real system is free of noise. A better understanding of the types of noise present in a system allows the design of a controller with better noise immunity. For the VCUUV there are two primary sources of noise which need to be characterized, power converter noise and quantization error.

The power converters used on the VCUUV are dc-dc switching power supplies, which produce the various voltages required by the on-board circuitry. They have an internal switching frequency of approximately 20kHz and produce high-frequency electromagnetic radiation throughout the vehicle, inducing currents in anything that conducts electricity. This includes, unfortunately, the electronics on the signal-conditioning board. This adds noise which is of a fairly wide spectrum to the signals going into the analog-to-digital converters. The frequencies present in this noise are all well above the Nyquist rate of the sampling circuitry, so the sampled version of the signal has aliased noise at all frequencies. For the purposes of modeling, it is not unreasonable to regard this as band-limited white noise although a mathematical proof of this is beyond the scope of this thesis.

It is helpful to know what the amplitude of a noise source is in addition to knowing its frequency content, so that general predictions about its effect on control performance can

be made, and appropriate filters designed if necessary. It is easier and more accurate to measure the amplitude of this noise directly rather than attempt to predict it mathematically. The amplitude of the noise on a typical analog-to-digital converter input in the VCUUV is about 10-15 quanta, which introduces about 1% error for position measurements.

When an analog signal is converted to a digital one, as is typical required in a discrete-time controller, a tiny amount of error may be introduced due to quantization. Oftentimes is convenient to model this error as a white noise source, but this model breaks down if the signal is not continuously varying.

The position signals in the VCUUV are not necessarily varying all the time, so the effects of quantization simply set the limit on how accurately the tail can be positioned. With the twelve bits of resolution in the analog-to-digital converters, the position of the tail can be measured to the nearest hundredth of a degree, which is more than sufficient. Because of this, the effects of quantization can safely be ignored.

4. Linear Position Control Techniques

For a wide variety of systems, a linear proportion-integral-derivative controller provides perfectly adequate performance.

This chapter describes the design of several types of linear controllers and discusses the various limitations of each. This chapter also discusses the issue of selecting the appropriate sampling rate for a discrete-time control system.

4.1. Proportional Control

Because proportion control is so easy to implement, it was the first controller designed for the VCUUV. The simulations of the proportional controller indicate that while it would be adequate for demonstrations and development purposes, the error would never be small enough to provide the level of accuracy required.

The basic structure of the proportional controller is shown here in Figure 4-1.

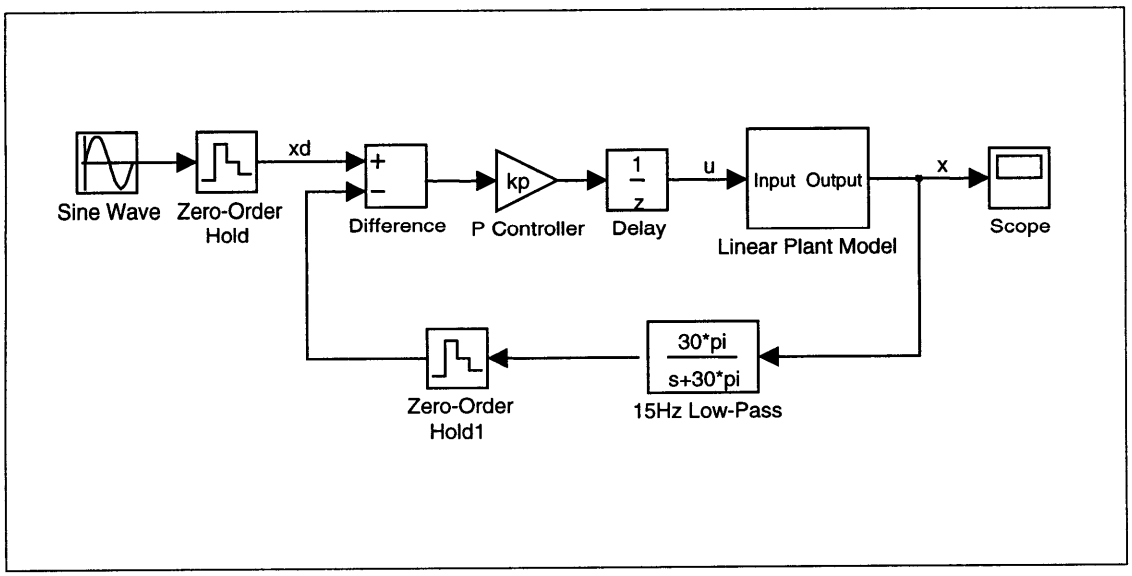

Figure 4-1 Block Diagram of Proportional Controller

The problem with this type of control system is that it can never achieve perfect tracking. This is easy to see from the control law

$$u = k_p \times \tilde{x}$$

(4.1)

For x_d to be tracked perfectly, $\tilde{x}$ must be zero. If x_d is time-varying, then x and thus u must also be time-varying. But (4.1) says that if $\tilde{x}$ is zero, u will also be zero. So $\tilde{x}$ cannot be zero if x_d is time-varying, and hence this controller cannot track time-varying signals without error.

This controller has only one parameter that can be adjusted, k_p, the proportional gain. The value of this parameter is selected to minimize phase-lag of the response to a sinusoidal input of 1.4Hz, without affecting the magnitude of the response adversely. The value of k_p for which this occurs can be calculated directly by requiring that the poles of the discrete-time closed-loop system lie on the real axis, and minimizing their magnitudes. The resulting equations for this technique are not provided here as it is typically much easier to arrive at the optimal value for k_p by iteratively refining a guess until the previously mentioned conditions are met. The bode function of MATLAB is particularly useful for this process.

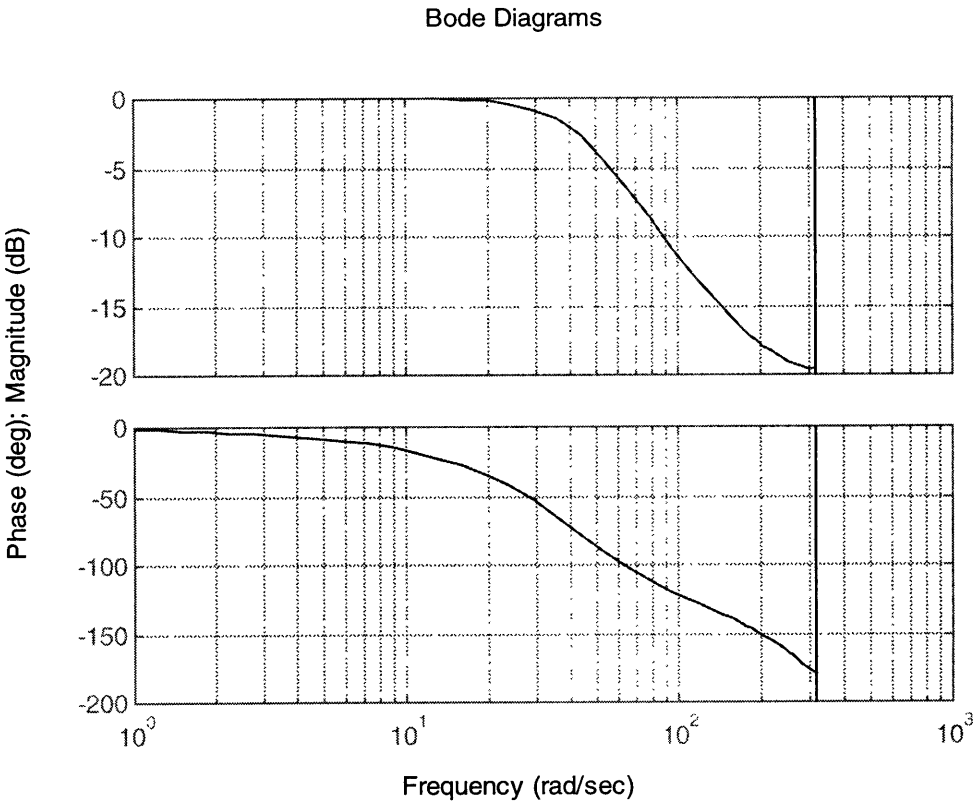

Figure 4-2 Closed-Loop Response of Proportional Controller

Figure 4-2 show the Bode plots of magnitude and phase for an optimally tuned proportional controller operating at a sampling rate of 100Hz. The value of *kp* used to generate this plot was 22. The graph shows fairly flat magnitude response out to 1.5Hz (9.4 rad/s). It shows, however, marked phase-lag at that frequency.

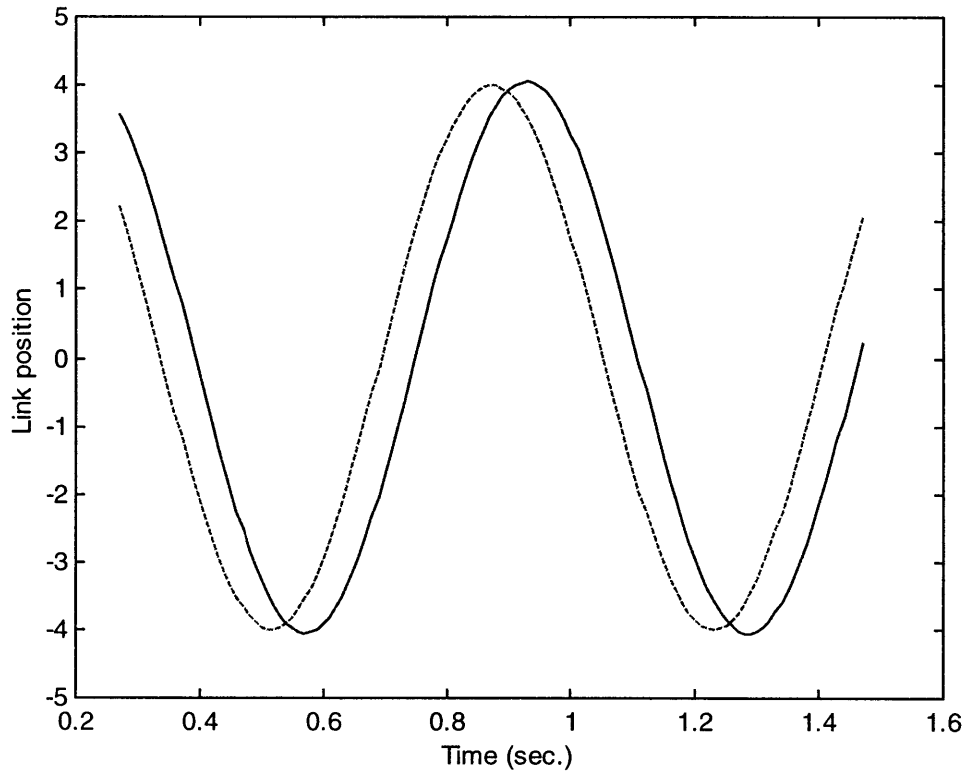

Figure 4-3 Simulation of Proportional Controller with Sinusoidal Input

Figure 4-3 shows the simulated response of a proportional controller as it tracks a sinusoidal input of 1.4Hz.

Recalling the robustness requirement of Chapter 2, the question is raised: how well will the system perform when the cylinders are loaded with the mass of the water? Examining (3.10) it can be seen that as the load on a particular cylinder increases, the gain of the controller is effectively reduced. This inspires an examination of the root locus diagram for this system, seen in Figure 4-4.

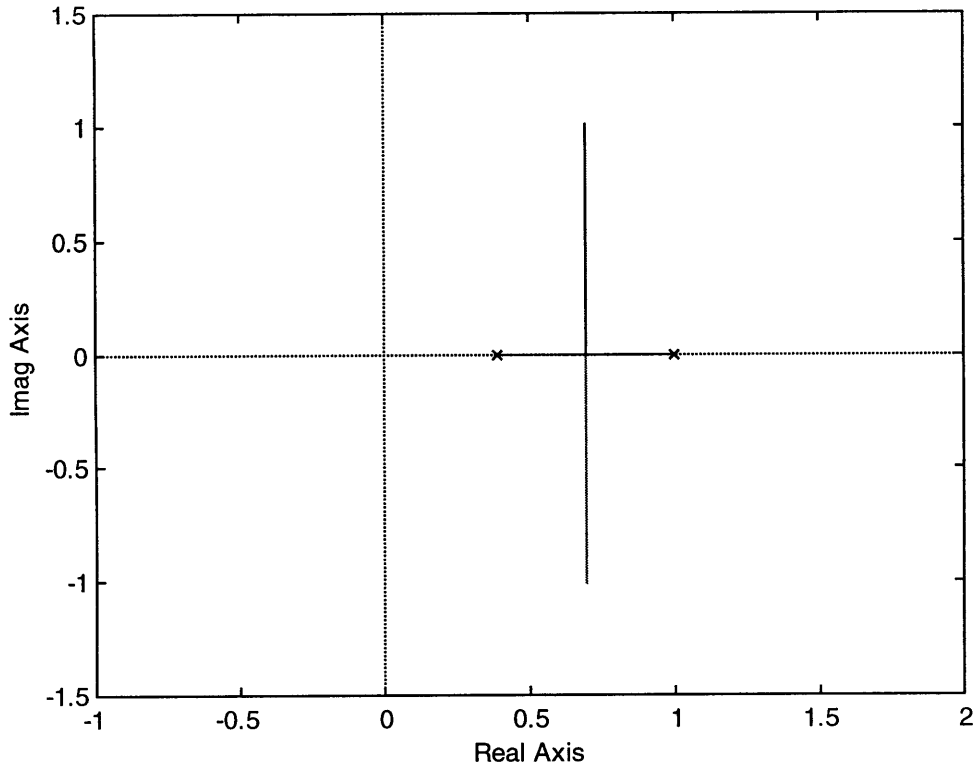

Figure 4-4 Root Locus Diagram

The root locus diagram shows that for positive values of k_p below a certain value, the roots of the loop transfer function remain within the unit circle. This means for constant levels of loading less than the stall load, the system is guaranteed to remain stable.

For time-varying loads, as will generally be present during normal operation, a Simulink model confirms the continued stable operation of the system. Figure 4-5 shows a graph of the simulated system response to a 1.4Hz sinusoid under sinusoidal loading conditions. The peak loading in this example is approximately 70% of the stall load. The results of this simulation suggest that this controller is reasonably robust.

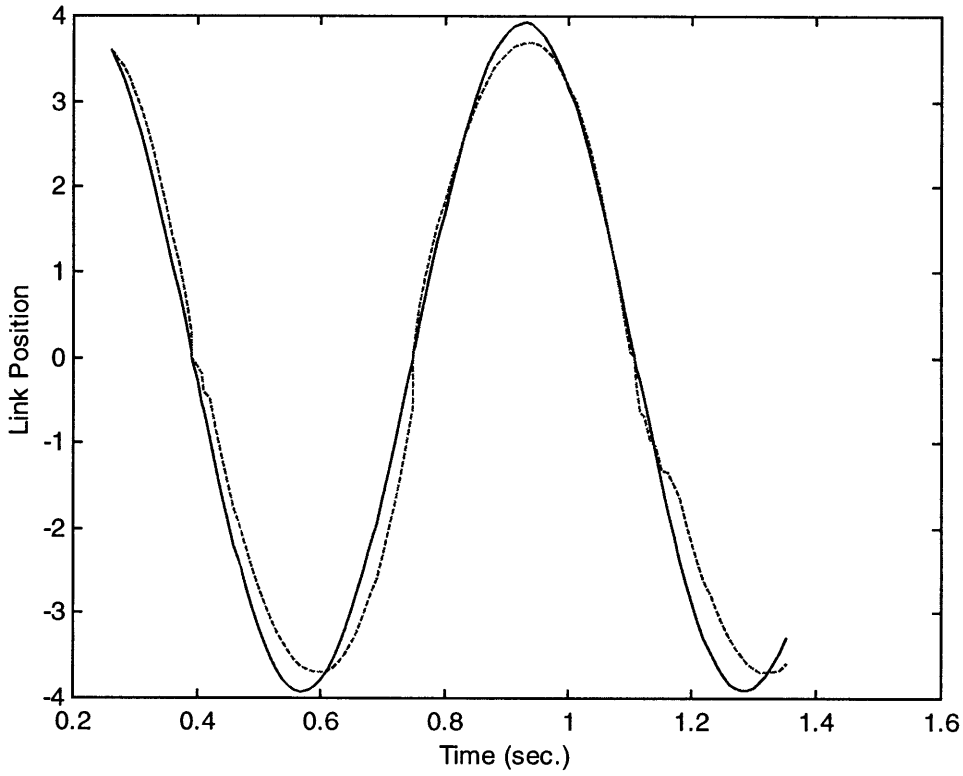

Figure 4-5 Simulation of Tracking Under High Loading Conditions

4.2. Perfect-Tracking Proportional Control

A more interesting type of controller is the perfect-tracking proportional controller. Unlike the proportional controller, which by design must always have some error, it is possible for the perfect-tracking proportional controller to have no error, even in response to time-varying input trajectories. The block diagram of such a controller is shown in Figure 4-6.

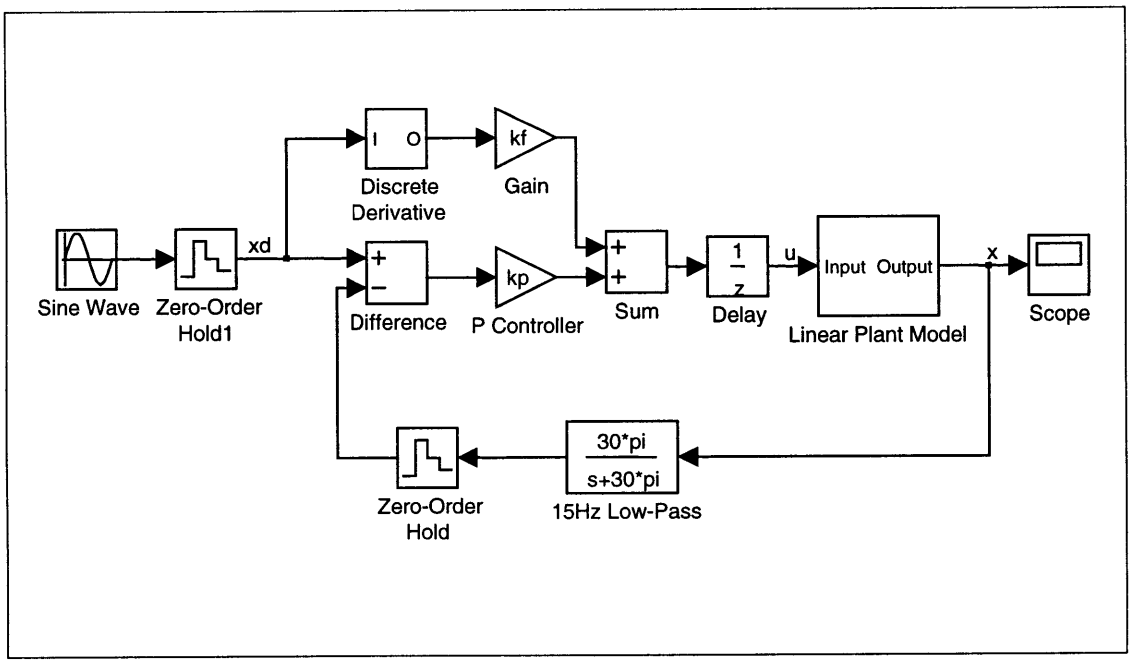

Figure 4-6 Block Diagram of Perfect-Tracking Controller

In order to provide perfect tracking, the inverse of the plant model is placed on a feed-forward branch of the controller. As the linear plant model is an integrator, the derivative of the desired trajectory is added into the control effort. If the model for the plant were perfect, then the error could be zero for all time. The feed-forward branch would supply the exact control effort required and the system would have perfect tracking. Of course, this doesn't happen because of model deficiencies, disturbances, and noise.

In this controller there are two parameters to vary, k_f and k_p. In the case of a continuous time controller, the selection of these values is very straightforward. Since the feed-forward path is ideally the inverse of the plant model, k_f is set to 1, assuming the plant model has been normalized. As the system is guaranteed to be stable for all values of k_p, it can be set as high as is necessary to meet the bandwidth requirements.

Since the VCUUV is being controlled by a discrete-time controller, the values for k_f and k_p must be chosen more carefully. The dynamics of the zero-order hold and the computation delay place upper bounds on the loop gain. The value of k_p controls the level of disturbance rejection for this controller, so it is desirable to set it as high as possible. As k_f approaches 1, the system approaches operation with zero tracking error.

A reasonable algorithm for setting these gains appropriately is to first determine the maximum value of k_p which does not result in an increase in amplitude for a 1.4Hz sinusoidal input, just as in Section 4.1. Next, set k_f to 1 and then reduce its value until error is minimized. This process is facilitated by the use of the Simulink package for MATLAB. The optimal values for k_f and k_p depend on the sampling period, T_s, used in the discrete-time controller.

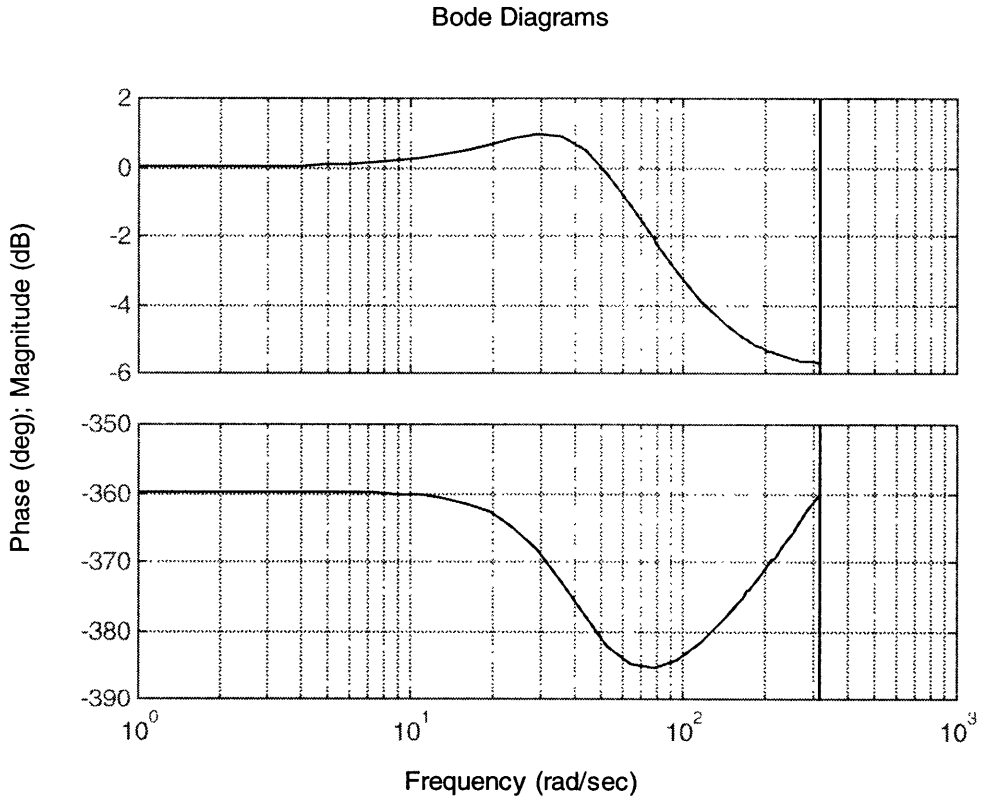

Figure 4-7 Closed-Loop Response of Perfect-Tracking Controller

Figure 4-7 shows the Bode plots of magnitude and phase for an optimally tuned perfect-tracking proportional controller operating at a sampling rate of 100Hz. The value of k_p used to generate this plot was 22, and the value of k_f was .6635. The magnitude response of this control system is not as flat out to 1.5Hz as the strictly proportional controller. It shows, however, greatly reduced phase-lag, as compared to the proportional controller.

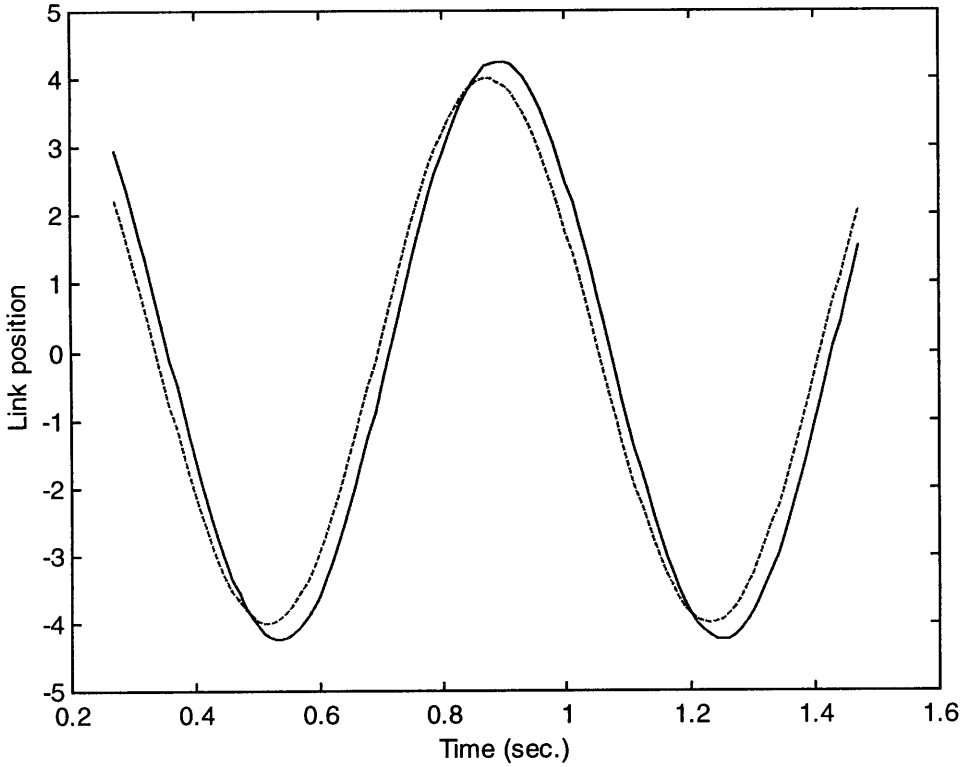

Figure 4-8 Simulation of Perfect-Tracking Controller with Sinusoidal Input

Figure 4-8 shows the simulated response of a proportional controller as it tracks a sinusoidal input of 1.4Hz. At this frequency the amplitude has started to peak up, however, the phase-lag is greatly reduced, and overall tracking is much improved.

As the closed-loop portion of the perfect-tracking controller is identical to that of the proportional controller, the robustness of the stability and disturbance rejection are the same as for the strictly proportional controller.

4.3. Time-Varying Linear Control

In developing the linear model for the hydraulic system, the high-pressure accumulator pressure, P_h, was assumed to be a constant, held so by a separate control loop. In reality, it is unlikely that the pressure control loop will be able to maintain P_h at a constant value.

If the fluctuations in P_h are great enough, it could have an adverse effect on control system performance.

To correct for this, the measured instantaneous value of P_h can be used to rescale the control effort. Specifically, the control effort is divided by $\sqrt{P_h}$. This technique can easily be combined with any of the linear control systems described in this chapter.

One complication with this technique is the possibility of division by zero. A simple solution to this problem is to always check that P_h is still above a certain predefined level before using it to rescale the control effort.

4.4. Sampling Rate Selection

The performance of a discrete-time control system generally only improves as the sampling rate increases. The disadvantages of higher sampling rates include increased hardware costs and increased computational demands. Also, if a discrete-time derivative is used, higher sampling rates result in greater amplification of noise.

In the case of the VCUUV, there is a dedicated processor for the control system so any unused computational power is wasted. Based on software profiling information, it was determined that the theoretical highest possible sampling rate is 500Hz. This figure could become smaller if the complexity of the software implementing the control system increases, so to make allowance for future changes, the sampling rate was set to 400Hz. The issue of the discrete-time derivative is addressed by including a low-pass filter whenever a discrete-time derivative is used. This filter removes the high-frequency noise introduced by the derivative.

5. NONLINEAR POSITION CONTROL TECHNIQUES

One of the primary advantages of the discrete-time controller is the ease with which nonlinear control schemes can be implemented. This chapter discusses a couple of simple nonlinear control techniques which can be used in conjunction with a linear control system such as the ones described in Chapter 4.

5.1. Servovalve Dead Spot Compensation

When a servovalve is commanded to its zero position, in theory, no fluid will flow in either direction through either of the orifices. In actuality there is always a tiny amount of leakage. When the servovalve is near its zero position there become four tiny orifices instead of just two, and it is then possible for fluid to leak directly from the high-pressure accumulator to the low-pressure accumulator without passing through the cylinder first. This effect creates a dead spot, where tiny deviations from the zero point do not actually result in any change in response on the part of the hydraulic system. Servovalve dead spot compensation works to alleviate the effects this has on system performance.

Servovalve dead spots result in a minimum speed at which the link can move without stopping completely. This causes the peaks and troughs of sinusoidal waveforms to be flattened out. It also results in non-zero steady-state error, despite the fact that the linear system model has a pole at zero. Both of these effects are undesirable.

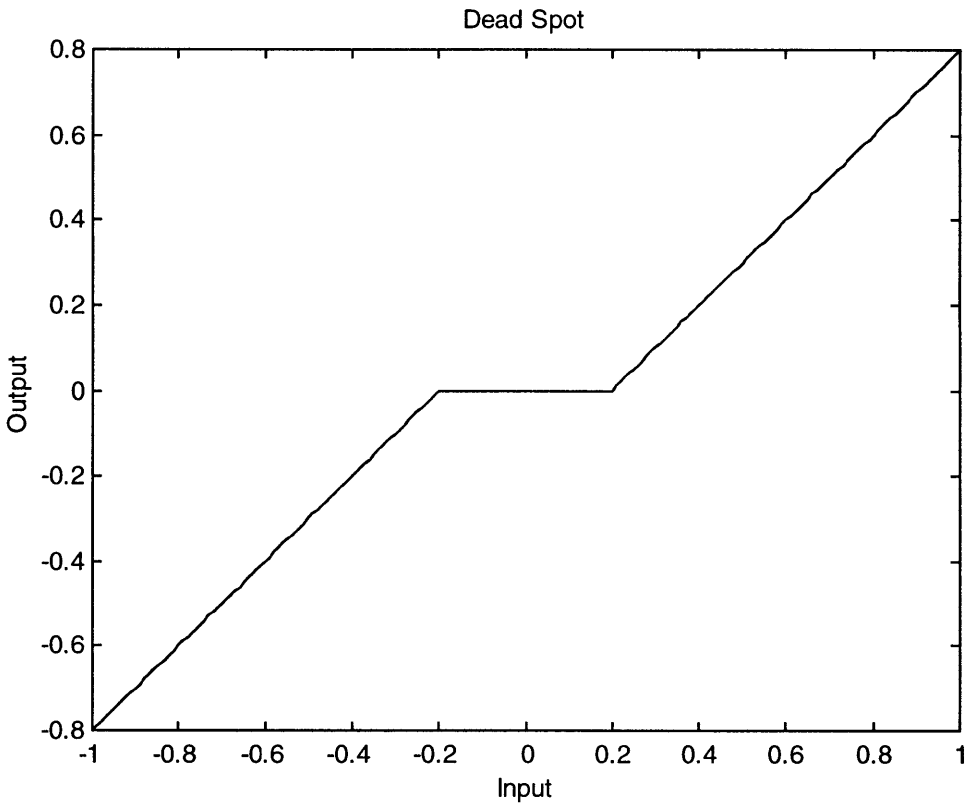

Figure 5-1 Input-Output Graph of Dead Spot

The solution to this problem is easiest to understand by examining a graph of a dead spot, shown in Figure 5-1. By graphically taking the inverse of this nonlinear function, a control law can be developed which will eliminate the dead spot. This can be represented mathematically by

$$u' = u + k_c \, \mathrm{sgn}(u)$$

(5.1)

where u' is the compensated control effort, u is the uncompensated control effort, and k_c determines the amplitude of the chatter. Figure 5-2 represents this input-output relationship graphically, providing somewhat of an intuitive feel for why it works.

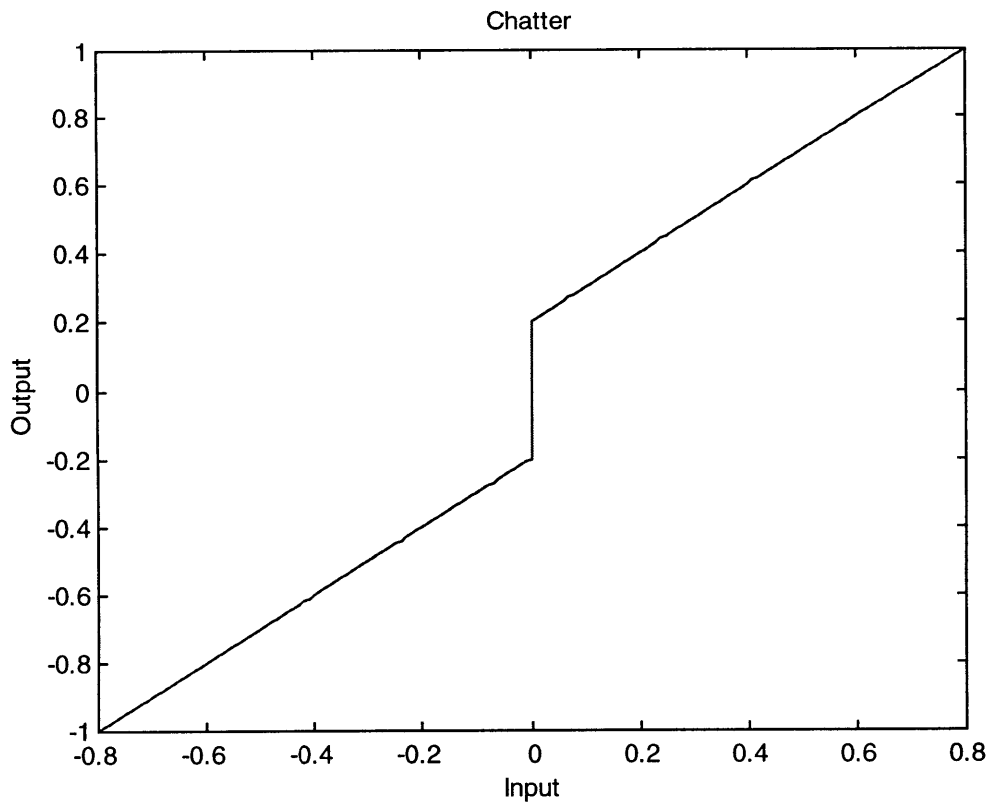

Figure 5-2 Input-Output Graph of Chatter

This sort of compensation introduces what is known as chatter, as it causes the control effort to oscillate rapidly back and forth around the zero point, whenever the uncompensated control effort is inside the dead spot region. For systems such as this one, this high-frequency chatter is filtered out by the natural low-pass filter characteristic of the plant, causing the plant to respond as if there were no longer any dead spot at all.

If the value of k_c is set too large, the amplitude of the chatter becomes large enough that it will more than compensate for the dead spot and cause needless high-frequency oscillations in the system response. If the value of k_c is set too low, then the effects of the dead spot are not be completely eliminated. When tuned properly, k_c is equal to half of the width of the dead spot.

Figure 5-3 shows a the output of a system with a dead spot, both uncompensated (the dotted line) and with properly tuned compensation (the solid line).

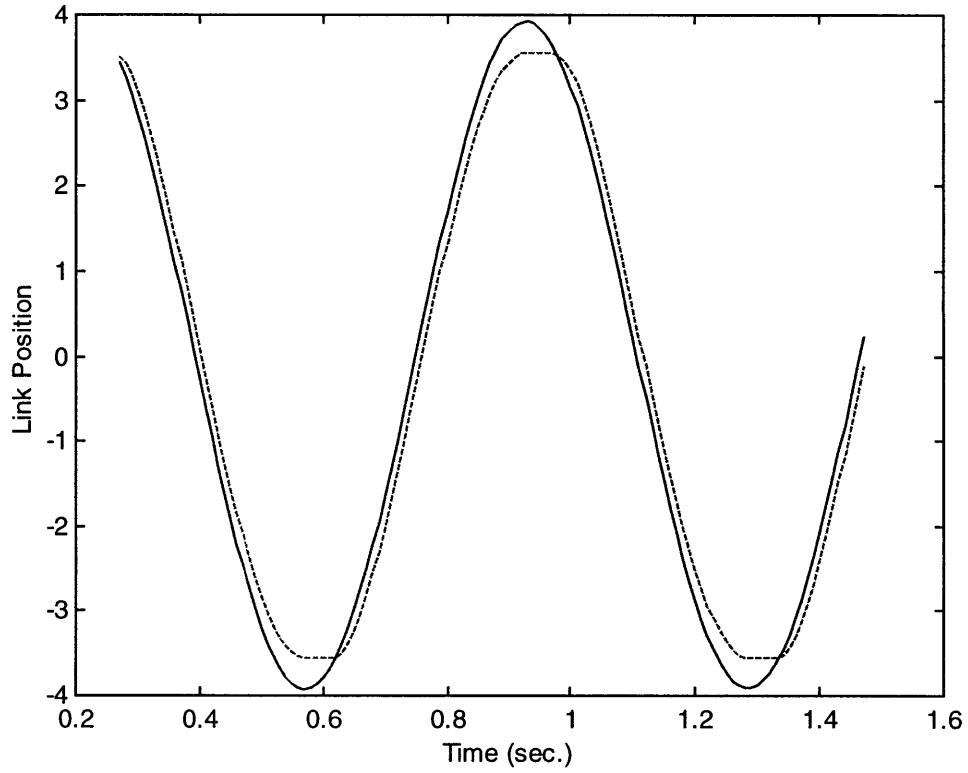

Figure 5-3 Simulation of System with Dead Spot with and without Compensation

5.2. Piston Area Compensation

In Section 3.3 it was shown that the difference in area between one side and the other of the piston in a cylinder creates an asymmetry around zero in the model of the hydraulic system. This asymmetry disappears when the pistons' areas are assumed to be equal, as in the development of (3.10). If, however, this approximation is relaxed, the need for separate control laws arises in order to provide symmetric performance.

Re-examining (3.9) it can be seen that simply scaling the control effort by different values depending on the sign of the control effort can correct for this problem if the cylinder loading is considered to be insignificant.

From (3.9) the appropriate rescalings are computed. Assuming the linear control law was developed using (3.11), the rescalings are given by

$$k_s = \begin{cases} \frac{A}{A1}\sqrt{\left(\frac{A2}{A1}\right)^2 + \frac{A2}{A1}} & u \geq 0 \\ \frac{A}{A2}\sqrt{\left(\frac{A1}{A2}\right)^2 + \frac{A1}{A2}} & u \leq 0 \end{cases}$$

(5.2)

where A is the average of $A1$ and $A2$ as in Section 3.3, and k_s is the rescaling factor. The control law is then compensated by

$$u' = k_s \times u$$

(5.3)

where u' is the compensated control effort and u is the uncompensated control effort.

Figure 5-4 shows a simulated system response for a system with piston area compensation (the solid line) and without (the dotted line). The ratio of the piston areas for this graph is 3:1, an exaggerated figure selected to make the effect easy to see.

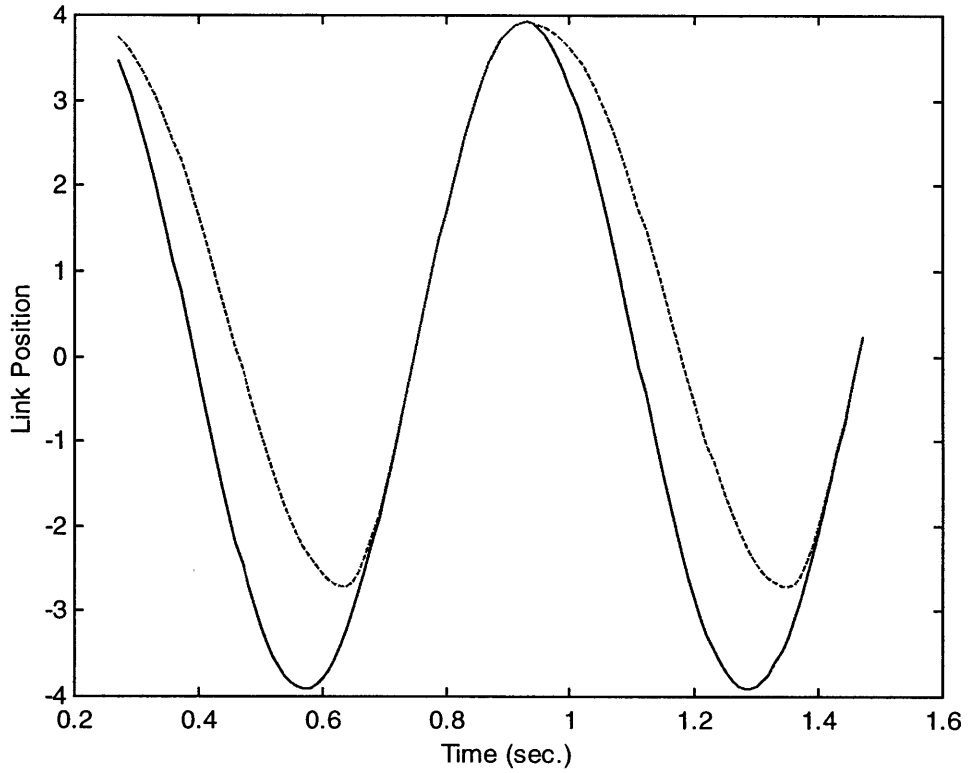

Figure 5-4 Simulation of System with and without Piston Area Compensation

5.3. Load Compensation

So long as the loading on a particular cylinder is light compared to available hydraulic pressure, the linear model of the hydraulic system developed in Section 3.3.2 will hold. It may be convenient for efficiency reasons to operate the VCUUV at lower hydraulic pressures than permitted by the assumption that $f/A \ll P_h$. In this section, a nonlinear technique for compensating for high loading conditions is examined.

If the assumption that $f/A \ll P_h$ is relaxed but the instantaneous value f is known, it is still possible to eliminate tail dynamics from the model. Essentially, when a cylinder is heavily loaded, a larger servovalve command is required to achieve the desired flow rate. By examining (3.10) such a control law can be established. To compensate for load the control effort is scaled by the square root of P_h over P_h minus f/A. This gives

$$u' = u \times \sqrt{\frac{P_h}{P_h - \frac{f}{A}}}$$

(5.4)

This reduces to the normal control law in the case where the loading is small enough that f can be ignored.

The fundamental difference between this technique and the time-varying linear control technique described in the previous chapter is that f is affected by u, making this nonlinear, whereas P_h can be generally considered to be independent of u.

6. CONTROL SYSTEM PERFORMANCE ANALYSIS

After designing and implementing a control system, it is interesting to compare the anticipated system performance with the actual system performance. Not only does this provide an indication of how well the system was modeled, in many cases the performance can be improved by adjusting various control parameters, either manually or automatically, as with an adaptive controller.

In the case of the VCUUV, the actual system response differed quite a bit from the modeled system response in some cases and followed the modeled response very closely in other cases. This chapter presents the results of the control system testing and discusses how the approximations made in previous chapters account for the differences between the modeled system performance and the actual system performance. The code for each of the controllers discussed in this section can be found in Appendix B.

6.1. Linear Control

The proportional controller and perfect-tracking proportional controller were tested both with the vehicle in air and with the vehicle in water. The proportional controller did not perform at an acceptable level. The perfect-tracking proportional controller worked very well for most of the links but showed very poor performance for one of the links.

6.1.1. Proportional Control

The straight proportional controller was the first type of control implemented because of its extreme simplicity. The proportional gain constants for each link were set to experimentally chosen values, with an emphasis on ensuring stability. As such, the gains were set lower than they should have been, and as a result, the tracking performance was quite poor.

Exact data is not available, but each of three links and the caudal fin showed on the order of 60 degrees of phase-lag. The amplitudes of the three links and caudal fin were very close to their commanded values when operated in air. However, when operated in water, the caudal fin showed attenuation to about 80% of its commanded amplitude. This performance level was unacceptable and prevented study of propulsive efficiencies. It did, however, propel the vehicle.

6.1.2. Perfect-Tracking Proportional Control

The perfect-tracking proportional controller was implemented and tuned as described in Chapter 4. Initial in-air testing of this controller provided very promising results. The tracking errors for in-air operation were on the same order as the signal noise and thus considered insignificant.

When the controller was tested in water, the results were not as favorable. Links one, two, and four (the caudal fin) performed very well. Link three, however, had serious tracking problems. The overall position-tracking ability of the tail was inadequate and again prevented the study of swimming efficiency.

Figure 6-1 shows both the desired (dotted line) and the actual (solid line) trajectories for link one. The nature of the tracking error is interesting to note. First, the leading edges of the peaks and troughs of the sinusoid are trimmed a bit. This effect is presumably due to the large forces acting against the cylinder during these periods of time. Another interesting aspect of this waveform is its asymmetry, caused by the difference in piston surface area as discussed in Section 5.2. These results suggest that the tracking error could be reduced by an appreciable amount if the techniques described in Sections 5.2 and 5.3 were applied.

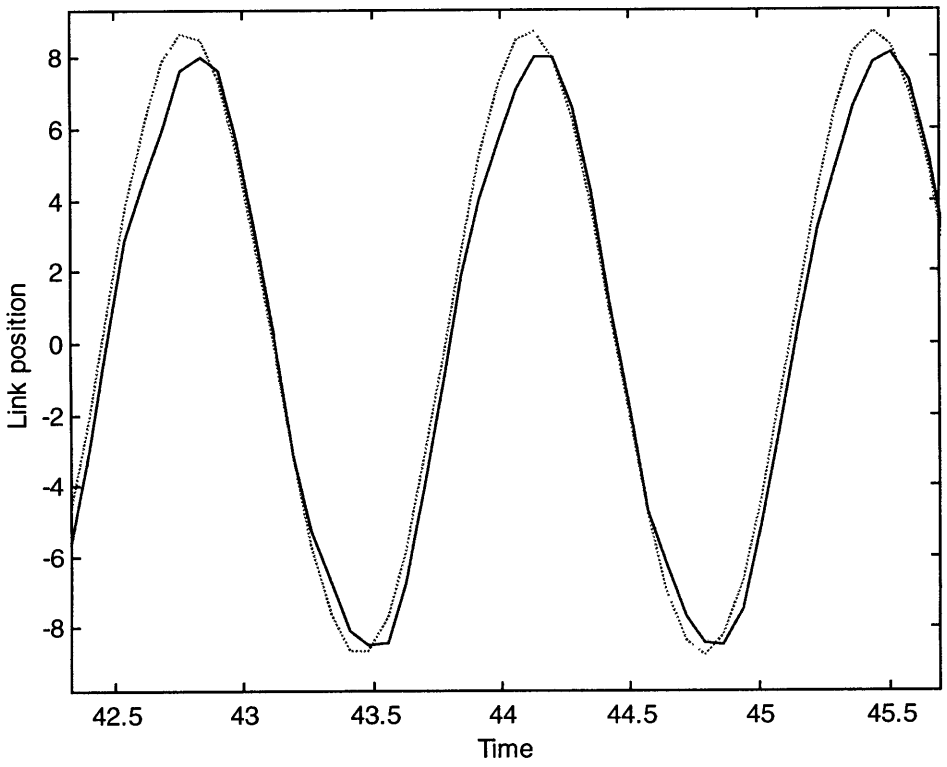

Figure 6-1 Actual and Desired Trajectories for Link #1

Figure 6-2 shows the actual (solid line) and desired (dotted line) trajectories for link three during the same test. The results are dramatically different. In this case, there are nearly 90 degrees of phase-lag. There is also a fairly drastic asymmetry, presumably due to the difference in piston surface areas. Also, the amplitude of the signal has been scaled up approximately 10%.

In order to understand what went wrong with link three, it is helpful to examine the load data for link three. Figure 6-3 shows a graph of this information. The exact waveform of this loading is not as interesting as its peak amplitude. The theoretical maximum force which link three can provide when the hydraulic system is operating at 600 psi is 113lbs. The load information shows that link three is being loaded very nearly to capacity. The excessive loading causes the linear model around which this control system was designed to break down. Thus, it is not surprising that system performance is so poor.

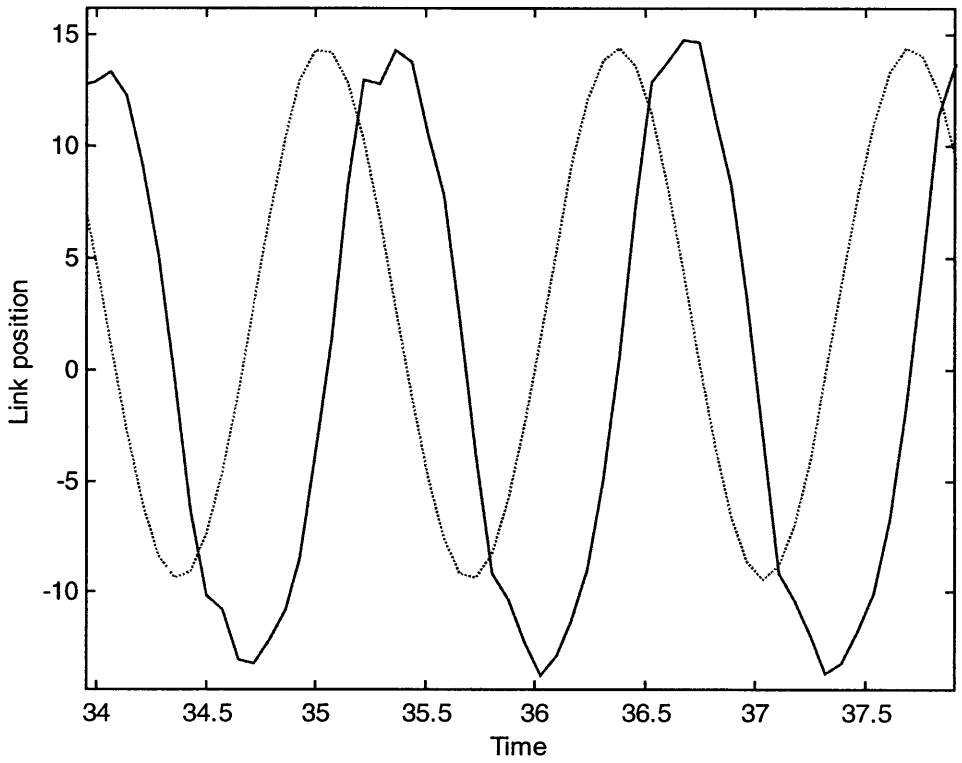

Figure 6-2 Actual and Desired Trajectories for Link #3

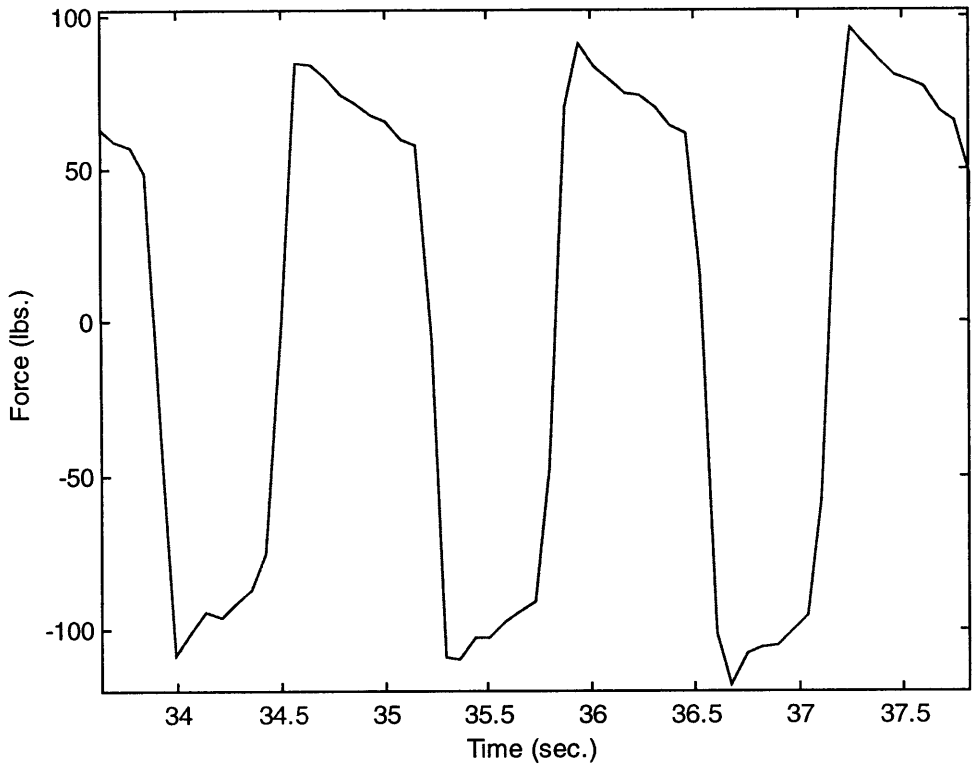

Figure 6-3 Loading on Link #3

6.2. Nonlinear Control

Unfortunately, time constraints have not allowed a thorough testing of the nonlinear control techniques described in Chapter 5. The servovalve dead spot compensation and piston area compensation techniques have not been tested yet, but the load compensation technique, perhaps the most interesting of the three, was tested out in an attempt to correct the problems with link three.

In seemed that if high loading conditions were the cause of the problem, that load compensation would be the ideal technique. Unfortunately, it appears that link three is not just heavily loaded but overloaded rather. When load compensation was employed, the tracking error showed only slight improvements. The control effort was found to be saturating under these conditions, however, suggesting that no control law would be able to bring the tracking error down to an acceptable level. The solution to this problem is,

unfortunately, a partial redesign of the hydraulic system and/or upgrade of pump motor control hardware.

7. CONCLUSION

This chapter summarizes the work completed and discusses areas for future research.

7.1. Summary of Work Completed

Over the course of this research several advancements in the control systems of VCUUV were made. A detailed model of the hydraulic system was developed. A control system which promises to provide acceptable performance has been created and tested. Because the hydraulic system is under-powered, the suitability of the controller developed cannot be confirmed at this time. Once the hydraulic system has been upgraded, it will be possible to confirm the fitness of the control system.

7.2. Directions for Future Research

Despite the significant progress made so far, the VCUUV project is far from complete. Just in the area of control systems there are several projects remaining. Closed-loop control of heading, speed, and depth, based on information from the navigation system, must be developed. More work can be done on controlling the pressure in the hydraulic system, focusing on increasing the efficiency of the pump and reducing the variations in hydraulic pressure.

In the area of tail control systems there are several topics for continued study. These include reducing sensor noise levels, applying adaptive control systems, and exploring the use of force control.

7.2.1. Noise Filtering

The noise levels in the sensor readings are fairly high, and better control performance could be achieved if this were corrected. There are a couple of angles from which to approach this problem, one largely a hardware project and one largely a software project.

The signal-conditioning hardware could be redesigned from scratch. A lot more about the requirements and challenges of this circuit is known now compared to when the circuit was originally designed. This additional knowledge could result in a superior design.

Another approach would be to analyze the noise to correct the problem. Once the power spectral density of the noise is analyzed, digital filters which reduce the noise levels can be designed. These filters can be developed such that they do not adversely affect control system performance.

7.2.2. Adaptive Control

Many of the parameters in the control systems described in the preceding chapters are based on approximations or iterative design techniques and are not necessarily set to their optimal values. The use of an adaptive controller could tune these parameters to their optimal values automatically.

7.2.3. Force Control

Instead of controlling the position of a link, a control system could be designed to control the force which a link applies to its surroundings. This system could then be used to simulate tail dynamics in software. For example, if the force applied by the link were constrained to be always in proportion to the position of the link, this would simulate the addition of a spring to that particular link. This technique could potentially aid in the design of a tail which relies on carefully tuned mechanical dynamics to increase its efficiency.

7.3. Conclusion

This thesis has described the development of the control system for tail of the VCUUV. As development of the VCUUV progresses, new and exciting things will be learned. The research community can look forward to new advances in propulsive efficiency and underwater vehicle maneuverability.

APPENDIX A: GLOSSARY

Caudal fin – The large fin at the end of the tail of a fish. It is the primarily source of propulsive force.

Neutrally buoyant – Having an average density equal to that of water, and thus neither floating nor sinking when submerged.

Plant – The physical system which is controlled in a control system. It typically is the portion of the system which is taken as a given, and around which a controller is designed.

Stall-load – The amount of force required to stop a hydraulic cylinder.

Steady-state error – The constant tracking error present in a control system when the desired trajectory is a constant value.

Tracking error – The difference between the desired trajectory and the actual trajectory of a control system.

Vorticity control – Controlling the formation of vortices to produce efficient propulsion. This is the technique that most fish employ.

APPENDIX B: CODE

This section is included for the benefit of the reader who is interested in the details of the actual implementations of the control techniques described in Chapters 4 and 5.

This function illustrates prefect-tracking time-varying proportional control with load compensation:

```
void control_control(const sensor *sensors, const float
   motion[TAIL_NUM_LINKS], float pressure, actuator *actuators)
{
   int i;
   float P,I,D,err,lead;
   static float lasterr[4],lastlead[4],lastinp[4][3]; /* Unitialized!!
   */
   float loopgain[4]={7.0872,6.3,6.3,2.8349};
   float fscale,fmotion,t1,t2,t3;
   static float derivtemp1old=0,derivtemp2old=0;
   float deriv1,deriv2,derivtemp1,derivtemp2;
   float Pc,a1,alph;

   if (control_mode==MANUAL_MODE)
   {
      /* In this mode, we just leave the servo settings alone */
   }
   else if (control_mode==PID_MODE)  /* PID control here */
   {
      for(i=0;i<TAIL_NUM_LINKS;i++)
      {
            /* First, we filter the input signal. */
            /* In assembly, this would take 5 clock cycles.  In C it
   will probably take 100. */

            fmotion=Igain[i]*(motion[i]-lastinp[i][0])*CONTROL_FREQ;
            lastinp[i][0]=motion[i];
            err=motion[i]-sensors->pos[i];

            P=Pgain[i]*err;

            Pc=Dgain[1]*sensors->load[i];

            if(sensors->pressure<200)
                  actuators->servovalves[i]=0;
            else
                  actuators->servovalves[i]=
   (fmotion+P)/(loopgain[i]*sqrt(sensors->pressure-Pc));

      }
   }
/* Before we return from control, let's bound the
      servovalve commands so we don't go beyond their
      saturation values */
   actuators->servovalves[0]=
      BOUND(ACTUATOR_SV0_MIN,actuators->servovalves[0],
```

```
      ACTUATOR_SV0_MAX);
   actuators->servovalves[1]=
      BOUND(ACTUATOR_SV1_MIN,actuators->servovalves[1],
      ACTUATOR_SV1_MAX);
   actuators->servovalves[2]=
      BOUND(ACTUATOR_SV2_MIN,actuators->servovalves[2],
      ACTUATOR_SV2_MAX);
   actuators->servovalves[3]=
      BOUND(ACTUATOR_SV3_MIN,actuators->servovalves[3],
      ACTUATOR_SV3_MAX);


   return;
}
```

APPENDIX C: VARIABLE DEFINITIONS

This section provides a concise listing of the variables used in this thesis and their meanings. Variables whose meaning depends on the context in which they are used are not listed here.

$A1$ – The smaller surface area of a piston.

$A2$ – The larger surface area of a piston.

A – The average of the two surface areas of a piston.

k_p – The proportional gain in a linear controller.

kf – The feed-forward gain in a linear controller.

x_d – The desired position trajectory for a controller to follow.

x – The actual position trajectory.

u – The control effort. In the case of the VCUUV, this is the servovalve command.

u' – The modified control effort. In Chapter 5, linear control laws are augmented by a nonlinear function of u, the control effort.

REFERENCES

1. Asada, Haruhiko and Jean-Jacques E. Slotine. 1986. *Robot Analysis and Control.* New York: John Wiley and Sons.

2. Cho, Jamie L. 1997. "Electronic Subsystems of a Free-Swimming Robotic Fish." M.Eng. thesis. Massachusetts Institute of Technology.

3. Nise, Norman S. 1995. *Control Systems Engineering.* 2nd ed. Menlo Park, CA: Addison-Wesley Publishing Company.

4. Oppenheim, Alan V. and Ronald W. Shafer. 1989. *Discrete-Time Signal Processing.* Englewood Cliffs, NJ: Prentice Hall.

5. Slotine, Jean-Jacques E. and Weiping Li. 1991. *Applied Nonlinear Control.* Englewood Cliffs, NJ: Prentice Hall.